doi:10.1038/nature06281

ARTICLES

Innate versus learned odour processing in the mouse olfactory bulb

Ko Kobayakawa[1]*, Reiko Kobayakawa[1]*, Hideyuki Matsumoto[2], Yuichiro Oka[1], Takeshi Imai[1], Masahito Ikawa[3], Masaru Okabe[3], Toshio Ikeda[4], Shigeyoshi Itohara[4], Takefumi Kikusui[5], Kensaku Mori[2] & Hitoshi Sakano[1]

The mammalian olfactory system mediates various responses, including aversive behaviours to spoiled foods and fear responses to predator odours. In the olfactory bulb, each glomerulus represents a single species of odorant receptor. Because a single odorant can interact with several different receptor species, the odour information received in the olfactory epithelium is converted to a topographical map of multiple glomeruli activated in distinct areas in the olfactory bulb. To study how the odour map is interpreted in the brain, we generated mutant mice in which olfactory sensory neurons in a specific area of the olfactory epithelium are ablated by targeted expression of the diphtheria toxin gene. Here we show that, in dorsal-zone-depleted mice, the dorsal domain of the olfactory bulb was devoid of glomerular structures, although second-order neurons were present in the vacant areas. The mutant mice lacked innate responses to aversive odorants, even though they were capable of detecting them and could be conditioned for aversion with the remaining glomeruli. These results indicate that, in mice, aversive information is received in the olfactory bulb by separate sets of glomeruli, those dedicated for innate and those for learned responses.

The mouse olfactory system can detect and discriminate diverse odorants using a repertoire of about 1,000 odorant receptor genes[1]. Each olfactory sensory neuron (OSN) expresses only one member of the odorant receptor gene family in a monoallelic manner[2]. Furthermore, OSNs expressing the same odorant receptor converge their axons to a specific set of glomeruli in the olfactory bulb[3]. Thus, odorous information received in the olfactory epithelium is converted to topographical maps of activated glomeruli. On the basis of the expression patterns of zone-specific markers[4,5], the olfactory epithelium can be divided into two, non-overlapping areas: a dorsal zone (D zone) and a ventral zone (V zone).

Vertebrate odorant receptor genes are phylogenetically divided into two distinct classes[6]: class I and class II. Class I odorant receptors are expressed exclusively in the D zone of the olfactory epithelium, and OSNs expressing them project their axons to the most antero-dorsal area in the olfactory bulb[7,8]. In addition to the class I odorant receptors, ~300 class II odorant receptors are also expressed in the D zone, but their corresponding glomeruli reside on the periphery of the class I area in the olfactory bulb. The remaining class II odorant receptors are expressed in the V zone and their glomeruli are found in the ventro-lateral area in the olfactory bulb[4,9]. Thus, the glomerular map seems to be subdivided into three compartments along the dorso-ventral axis in the olfactory bulb: a dorsal domain for class I odorant receptors (D_I domain), a dorsal domain for class II odorant receptors (D_{II} domain) and a ventral domain for class II odorant receptors (V domain) (Supplementary Fig. 1a). The olfactory bulb can also be divided into distinct domains in other ways, for example, on the basis of the chemical natures and structural features of odorous ligands[10]. Because a particular odorant interacts with many different odorant receptor species, multiple sets of glomeruli are activated in different olfactory bulb domains[11]. However, little is known about how the topographical information in the olfactory bulb is transmitted to and interpreted in the brain to decode the odour map. To address these questions, we generated two new strains of mutant mice in which the OSNs in a specific area of the olfactory epithelium are ablated.

Generation of the zone-specific depletion mice

We reported previously that the rat *Omacs* gene, encoding olfactory-specific medium-chain acyl-CoA synthetase, is expressed in the olfactory epithelium in a D-zone-specific manner before the onset of odorant receptor gene expression[5]. This was also confirmed in mouse by *in situ* hybridization and immunohistochemistry (Supplementary Fig. 2). We used the D-zone-specific *O-MACS* (also known as *BC048390*) promoter to ablate the D zone OSNs in mice (ΔD) by targeted expression of the diphtheria toxin gene[12]. We first generated a knock-in mouse strain in which the coding sequence of the *O-MACS* was replaced with that of the Cre-recombinase gene (*O-MACS→cre*). We then crossed this knock-in mouse with another mouse strain carrying the Cre-inducible *lacZ* gene. The *lacZ* reporter, activated by Cre that is driven from the *O-MACS* promoter, was selectively expressed in the D zone of the olfactory epithelium by embryonic day 11. No other tissues, including the brain, expressed *lacZ* (Supplementary Fig. 3). We thus confirmed the D-zone-specific induction of Cre. Next, we crossed the *O-MACS→cre* mouse with a knock-in mouse (*Eno2-STOP-DTA*) in which the Cre-inducible diphtheria toxin A gene (*DTA*) was introduced into the neuron-specific enolase gene (*Eno2*) locus (Fig. 1a, ΔD). D-zone-specific ablation of OSNs in the olfactory epithelium was confirmed by *in situ* hybridization and by polymerase chain reaction with reverse transcription (RT–PCR) analyses for various odorant receptors (Fig. 1b and Supplementary Fig. 1b, ΔD).

We also generated the class-II-depleted (ΔII) mouse using the olfactory receptor 16 (*MOR23*, also known as *Olfr16*) promoter. We obtained several lines of the *MOR23→cre* transgenic mice[13] and crossed them

[1]Department of Biophysics and Biochemistry, Graduate School of Science, The University of Tokyo, Tokyo 113-0032, Japan. [2]Department of Physiology, Graduate School of Medicine, The University of Tokyo, Tokyo 113-0033, Japan. [3]Research Institute for Microbial Diseases, The Osaka University, Osaka 565-0871, Japan. [4]Laboratory for Behavioral Genetics, Brain Science Institute, RIKEN, Saitama 351-0198, Japan. [5]Laboratory of Veterinary Ethology, The University of Tokyo, Tokyo 113-8657, Japan.
*These authors contributed equally to this work.

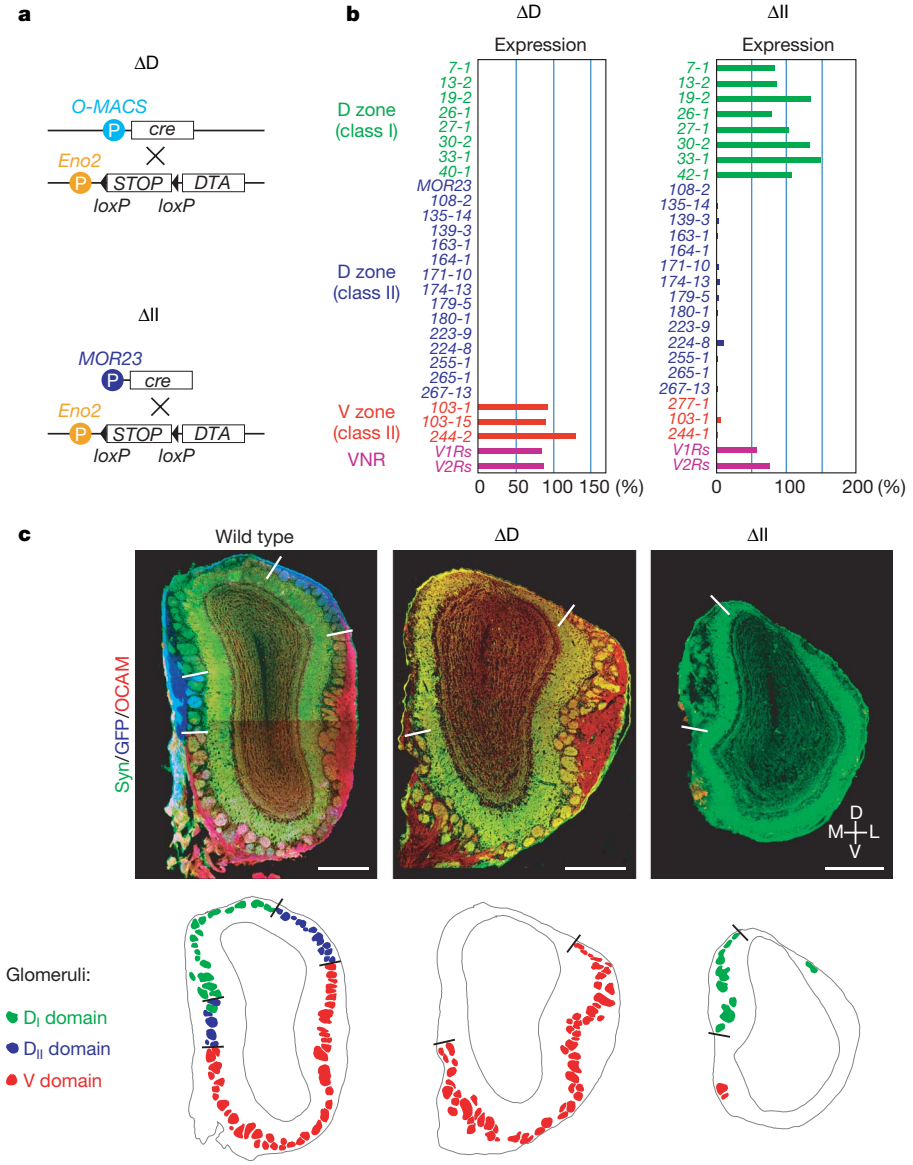

Figure 1 | Odorant receptor gene expression and glomerular map formation in the ΔD and ΔII mutant mice. **a**, Plasmid constructs for the D-zone depletion (ΔD) and the class II depletion (ΔII) are schematically illustrated. *DTA* and *cre* are the genes for diphtheria toxin A and Cre recombinase, respectively. **b**, Expression of the odorant receptor and vomeronasal receptor (VNR) genes. Olfactory epithelium sections dissected from the ΔD, ΔII and wild-type mice were analysed by *in situ* hybridization. The number of OSNs expressing a given receptor per unit volume of mutant olfactory epithelium was compared with that of wild-type control (%). In the ΔD mutant, OSNs expressing the D-zone-specific odorant receptor genes, both class I (green) and class II (blue), were ablated. In the ΔII mice, OSNs expressing the class II odorant receptor genes, in the both D (blue) and the V (red) zones, were ablated. Expression of the vomeronasal receptor genes (purple)—*V1Rs* (*V1re8*, *V1rg1* and *V1rj3*) and *V2Rs* (*V2r1b*, *V2r11* and *V2r15*)—was also analysed, and the mean ratios are shown. **c**, Coronal sections of olfactory bulbs. Samples were dissected from the mutant mice (ΔD and ΔII) and the wild-type mouse in which the class II odorant-receptor-expressing OSNs were labelled with GFP. Olfactory bulb sections were stained with anti-synaptotagmin (green, Syn), anti-GFP (blue) and anti-OCAM (also known as NCAM2; red) antibodies. Distributions of glomeruli are schematically shown below the images (D_I-, D_{II}- and V-domain glomeruli are illustrated in green, blue and red, respectively). Borders for D_I domains (GFP^-/$OCAM^-$) and D_{II} domains (GFP^+/$OCAM^-$) are indicated by solid lines. D, dorsal; L, lateral; M, medial; V, ventral. Scale bars, 500 μm.

with the *Eno2-STOP-DTA* mouse to ablate OSNs under the control of the *MOR23* promoter (Fig. 1a, ΔII). With one particular transgenic line, the depletion unexpectedly occurred throughout the entire class II region of the olfactory epithelium (Fig. 1b and Supplementary Fig. 1b, ΔII). *In situ* hybridization and RT–PCR analysis demonstrated that none of the class I odorant receptor genes was affected in this mouse (Fig. 1b and Supplementary Fig. 1b, ΔII), with the exception of two class I genes[8] expressed in the V zone (data not shown).

Arrangement of glomeruli in the olfactory bulb

We analysed the formation and arrangement of glomeruli in the mutant mice by immunohistochemistry (Fig. 1c and Supplementary Fig. 4). In the ΔD mouse, glomeruli were found only in the postero-ventral region of the olfactory bulb (V domain), leaving the antero-dorsal region (D domain) vacant (Fig. 1c and Supplementary Fig. 4, ΔD). This was also confirmed by imaging of intrinsic signals in the olfactory bulb. In contrast to the wild-type mouse, no odour-evoked activities were detected on the dorsal surface of the olfactory bulb in the ΔD mouse ($n = 3$) (Supplementary Figs 5a, 6 and 7). Despite the complete absence of glomeruli, the D domain of the mutant olfactory bulb showed otherwise normal cytoarchitecture with distinct layers (Supplementary Fig. 8a). Individual mitral cells in the D domain of the mutant olfactory bulb emitted several dendrites into the external plexiform layer, but did not form dendritic terminal tufts, suggesting that these mitral cells lacked synaptic inputs from OSN axons (Supplementary Fig. 8b, c). V-zone OSN axons did not form ectopic contacts with the D-domain mitral cells in the ΔD olfactory bulb. No glomeruli were found in the D domain in the ΔD mouse during the course of embryonic development (data not shown). These results indicate that mitral cells are specified as D-domain and V-domain subsets before the projection of OSN axons occurs. The D-domain mitral cells seem to be committed to receive olfactory inputs exclusively from D-zone OSNs.

We then analysed the ΔII mouse. In contrast to the ΔD mutant, the ΔII mouse had glomeruli only in the most antero-dorsal part of the D domain (Fig. 1c and Supplementary Fig. 4, ΔII). To determine the boundary of class I and class II areas in the wild-type olfactory bulb, a mouse containing the Cre-inducible green fluorescent protein (*GFP*) gene was crossed with the *MOR23→cre* mouse to produce a mouse in which class-II-expressing OSNs are labelled with GFP (class II-GFP). In the class II-GFP mouse, the D_I-domain glomeruli (negative for GFP) and D_{II}-domain glomeruli (positive for GFP) are segregated into two distinct areas in the D domain of the olfactory bulb, even though both types of D-zone OSNs are intermingled within the D zone of the olfactory epithelium[8] (Fig. 1c and Supplementary Fig. 4, wild type). In the ΔII mouse, glomeruli were found in the D_I domain, and were absent in the class II regions (D_{II} domain and V domain) of the olfactory bulb (Fig. 1c and Supplementary Fig. 4, ΔII).

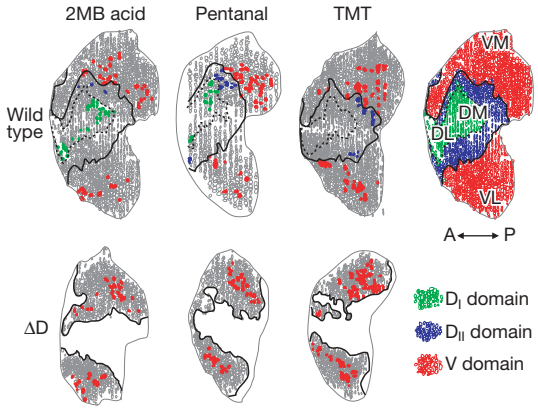

Figure 2 | Odour maps for aversive odorants. Unrolled maps for Zif268 expression. Glomeruli activated by 2MB acid, pentanal and TMT were detected by staining for the immediate-early gene product Zif268. Zif268-positive glomeruli are indicated in the unrolled olfactory bulb maps for wild-type and ΔD mice by three different colours: D_I (green), D_{II} (blue) and V (red). DL, dorso-lateral; DM, dorso-medial; VL, ventro-lateral; VM, ventro-medial.

Odour-activated glomerular maps in the olfactory bulb

A single odorant can interact with several different odorant receptor species and activate multiple sets of glomeruli in distinct areas in the olfactory bulb[11]. In rats, glomeruli for odorous ligands with similar odour characteristics tend to be clustered in the olfactory bulb[10]. This also seems to be true in mice (Supplementary Fig. 6). We analysed odour-activated glomerular maps by optical imaging of intrinsic signals[14–16] (Supplementary Figs 5a, 6 and 7) and by expression of Zif268 (also known as Egr1), an immediate-early gene product[17] (Fig. 2 and Supplementary Fig. 9). Three compounds were used: pentanal and 2-methylbutyric (2MB) acid, which are pungent odorants of spoiled foods, and trimethyl-thiazoline (TMT), which is secreted from the anal gland of fox[18] and induces aversive behaviour and fear responses in mice[19,20]. These odorants activate glomeruli in both D and V domains in the olfactory bulb (Fig. 2 and Supplementary Fig. 9). The 2MB acid activates glomeruli in the D_I and V domains; pentanal activates glomeruli in the D_I, D_{II} and V domains; and TMT activates glomeruli in the D_{II} and V domains. In the ΔD mouse, only V-domain glomeruli were activated (Fig. 2 and Supplementary Figs 5a and 9).

We then analysed the detection thresholds for these odorants by the habituation–dishabituation test[21] (Supplementary Figs 5b and 10). Comparing the ΔD mouse to the wild-type mouse, the detection thresholds for pentanal and TMT were not affected, whereas it was ten-times higher for 2MB acid. In this regard, it has been reported that, in rats, the most responsive glomerulus for pentanal is located in the V-domain area[22]. The same seems to be true in mice, not only for pentanal but also for TMT.

The ΔD mice fail to show innate avoidance behaviour

Rodents demonstrate avoidance behaviours towards predators' odorants[18–20]. They also avoid spoiled smells, for example, aliphatic acids[19,20], aliphatic aldehydes[23] and alkyl amines[24]. In contrast, rodents show attractive behaviours to food smells and conspecific odours[25]. We performed olfactory preference and avoidance tests with the wild-type and ΔD mutant mice.

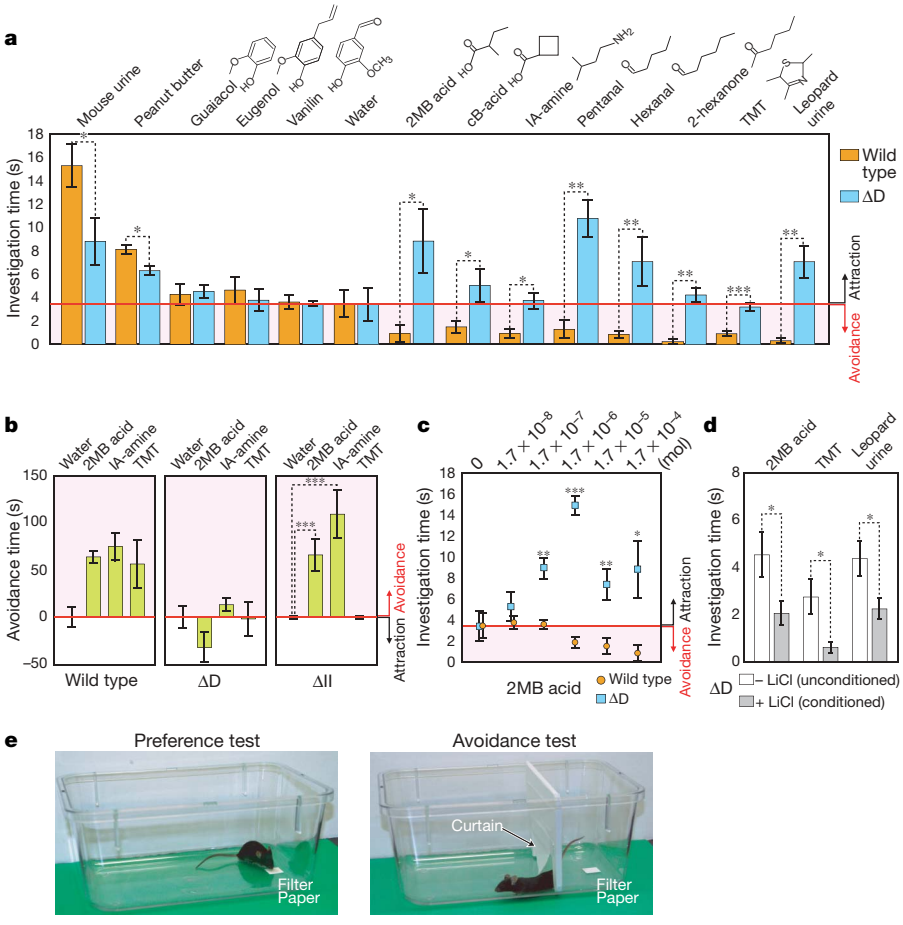

Figure 3 | Recognition tests for innate odour qualities. a, Innate olfactory preference tests. The duration for which the mouse investigated the scented filter paper was measured for various odorants. Mean investigation times (s) ± s.e.m. are shown for each odorant during the 3-min test period with the wild-type (orange) and ΔD (blue) mice. Investigation time for water was used as a criterion for attraction versus avoidance responses (red line). Investigation times less than this criterion (avoidance responses) are marked by the red shaded area. Asterisk, $P < 0.05$; double asterisk, $P < 0.01$; triple asterisk, $P < 0.001$. cB acid, cyclobutanecarboxylic acid; IA-amine, iso-amyl amine. **b**, Innate olfactory avoidance tests. Avoidance times were measured in a cage divided into two partitions (1:3) separated by a move-through curtain. The scented filter paper was placed in the smaller partition. During the 3-min test period, the time spent in the larger partition was measured as the avoidance time. Mean avoidance times (s) ± s.e.m. for test odorants relative to the mean avoidance time for water, which is set to 0, are shown as a bar graph. Triple asterisk, $P < 0.001$. **c**, Preference tests with the serially diluted 2MB acid. Mean investigation times (s) ± s.e.m. for 2MB acid in various amounts are plotted for the ΔD (blue squares) and wild-type (orange circles) mice. Asterisk, $P < 0.05$; double asterisk, $P < 0.01$; triple asterisk, $P < 0.001$ for a significant difference between investigation times of wild-type and ΔD mice for the same amounts of 2MB acid. **d**, Aversive conditioning of the ΔD mice. The ΔD mice were aversively conditioned to the indicated odorants with LiCl injection. Mean investigation times (s) ± s.e.m. are shown for each odorant during the 3-min test period for aversively conditioned (grey) and unconditioned (white) ΔD mice. Asterisk, $P < 0.05$. **e**, Photos of the preference (left) and avoidance (right) tests.

In the preference test (Fig. 3a and Supplementary Video), filter papers scented with various odorants were presented to the wild-type and ΔD mutant mice. The lengths of time the mouse spent investigating and sniffing the odorants were measured. Investigation times for wild-type mice were approximately 4 s for water (neutral odorant), within 0.3–1.3 s for acids, aldehydes, amines, ketones and predator odours, and 8–15 s for mouse urine and peanut butter. We used the investigation time for water (4 s) as a criterion for avoidance (shorter than 4 s) versus attraction (longer than 4 s) responses. In contrast to the wild-type, the ΔD mice spent a much longer time, 4–10 s, investigating acids, aldehydes, amines, ketones and predator odours. The failure of ΔD mutants to demonstrate avoidance behaviour was also confirmed by the innate avoidance test (Fig. 3b). We performed the innate-olfactory preference test using serially diluted 2MB acid (Fig. 3c). Wild-type mice demonstrated avoidance responses at higher concentrations of 2MB acid, but showed neutral behaviours at lower concentrations. In contrast, ΔD mice showed attractive behaviours at higher concentrations, and neutral responses at lower concentrations.

These results indicate that ΔD mice are able to detect 2MB acid, but fail to show avoidance behaviour. It should be noted that the mouse can be conditioned for aversive reactions by injection of irritating LiCl[26]. We used 2MB acid, TMT and snow leopard urine in the conditioning test, and found that the investigation time was significantly shortened after conditioning (Fig. 3d). It seems that ΔD mice can be conditioned for aversion, but they lack innately aversive responses.

The D zone is sufficient for innate avoidance behaviour

To examine the discrimination capabilities of the ΔD mouse, we performed an olfactory discrimination test[27] using four different pairs of odorants (Fig. 4). In this test, food-restricted animals were trained to associate either of the two related odorants to sugar rewards. After four days of training, the embedded sugar was removed from the test cage, and digging times for the two related odorants were compared within the same animal. It was found that ΔD mutants were able to discriminate 2MB acid, pentanal and (−)carvone from the competing odorants (cyclobutanecarboxylic acid, hexanal and (+)carvone, respectively). Mutant mice could discriminate even subtle differences between enantiomers as well as could wild-type mice. The wild-type mice could not be trained to associate TMT to sugar rewards, because the innate avoidance response was overwhelming. In contrast, the ΔD mouse easily discriminated TMT from eugenol, because the mutant did not avoid TMT.

To examine whether the D domain is sufficient to cause innate avoidance behaviour, we tested another OSN-ablated mutant, the ΔII mouse. The ΔII mouse demonstrated clear avoidance behaviours towards 2MB acid and iso-amyl amine, both of which activate D_I- and V-domain glomeruli (Fig. 3b). Interestingly, the ΔII mice did not avoid TMT, probably because the D-domain glomeruli for TMT are located exclusively in the D_{II} domain, which are absent in the ΔII mice (Fig. 2 and Supplementary Fig. 5a).

The innate fear pathway is not activated in the ΔD mouse

TMT activates the hypothalamic-pituitary–adrenal (HPA) axis in the rat brain, which has a significant role in regulating the adrenocorticotropic hormone (ACTH) level in response to stress[18,28]. Neurotoxic lesions of the lateral and basal nuclei of the rat amygdala do not prevent the TMT-induced freezing reaction[29]. Interestingly, muscimol (an agonist for a neurotransmitter, γ-aminobutyric acid A, $GABA_A$) does not block the TMT-induced freezing of rats when infused into the amygdala, but does block this reaction when introduced into the bed nucleus of the stria terminalis (BST)[30]. These observations indicate that the BST is involved in the TMT-induced fear processing. Using the immediate-early gene product Zif268 as a marker, we examined the TMT-induced activation of the BST (Fig. 5a, b). In the wild-type mouse, the BST was strongly activated in the medial aspect (BST-MA), and moderately in the lateral division (BST-LD). This is consistent with the previous observation that TMT activates the BST-MA, leading to the stimulation of the HPA axis in rats[28]. In contrast to the wild type, the BST-MA was not activated by TMT in the ΔD mice, although the BST-LD was activated as in wild-type mice. We also examined 2MB-acid-induced activation of the BST. In contrast to TMT, 2MB acid activated the BST-LD, but not BST-MA, in both wild-type and ΔD mice (Fig. 5a, b).

The HPA axis in rats, when activated by TMT, increases blood ACTH[28]. We measured the plasma concentrations of ACTH in both wild-type and ΔD mice (Fig. 5c). ACTH concentrations were found to increase significantly in the wild-type mouse, but not in the ΔD mutant, when TMT was present. These results indicate that the innate fear pathway in the ΔD mouse cannot be activated by TMT. With 2MB acid, the rise of ACTH was very small, if at all, even in the wild-type mouse (Fig. 5c). Although both TMT and 2MB acid cause avoidance responses in the wild-type mouse (Fig. 3a, b), only TMT activates the BST-MA and elevates plasma ACTH (Fig. 5a–c). These results indicate that fear responses induced by TMT and aversive responses to 2MB acid are separately processed in the brain with different neural circuits.

Discussion

In the present study, we generated zone-specific ablation mice, and studied glomerular map formation and odour perception in these mutants. When OSNs in specific olfactory epithelium zones were ablated, the corresponding olfactory bulb areas were devoid of glomerular structures. However, second-order neurons were present in

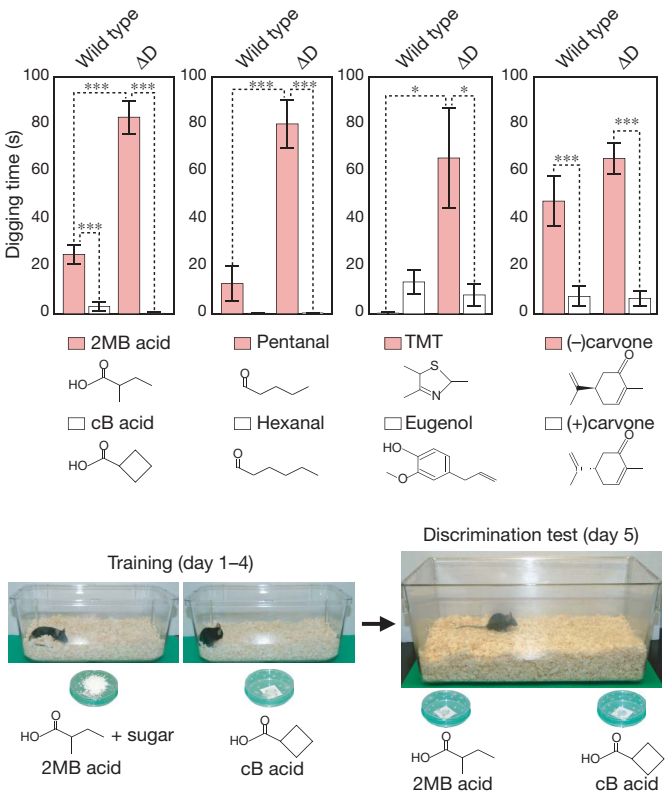

Figure 4 | Discrimination tests with structurally related odorants. The wild-type and ΔD mice were trained for four days to associate the reward (sugar grains) with either of the two related odorants. On day five, the sugar reward was removed from the bed, and digging times were measured for each pair of related odorants. Mean digging times (s) ± s.e.m. during the 2-min test period are shown as bar graphs for odorants paired with the sugar reward (red bars), and for unpaired odorants (white bars). Asterisk, $P < 0.05$; double asterisk, $P < 0.01$; triple asterisk, $P < 0.001$. Photos of the discrimination test are shown underneath.

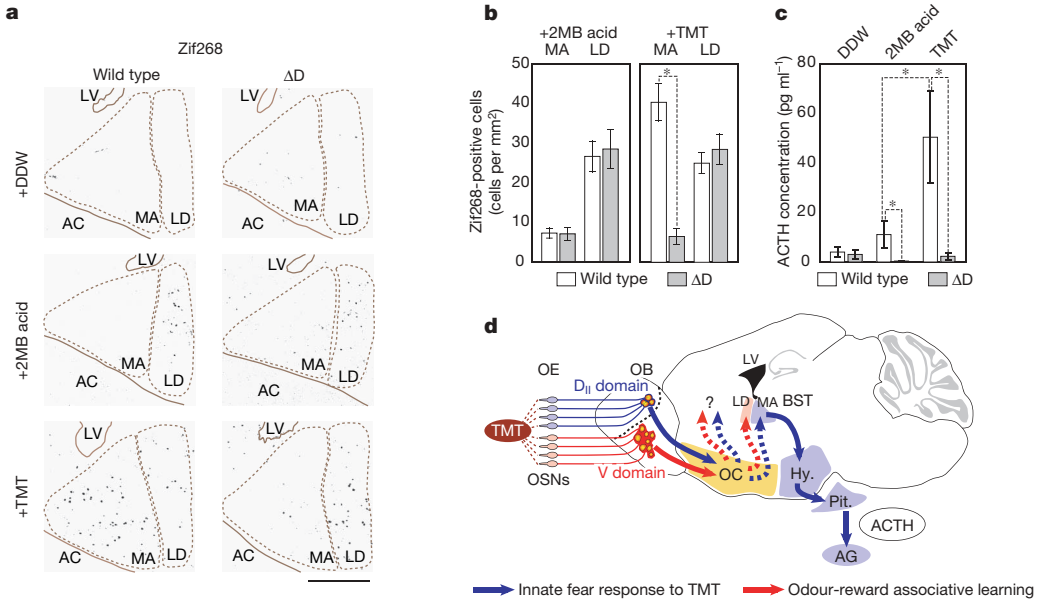

Figure 5 | 2MB-acid- and TMT-evoked neural pathways in the brain. **a**, 2MB-acid- and TMT-induced activation of the BST. The BST was activated by 2MB acid and TMT in the wild-type and ΔD mice. Double-distilled water (DDW) was used as a control. Coronal sections of the BST were immunostained with anti-Zif268 antibodies to detect the expression of the immediate-early gene *Zif268*. The lateral ventricle (LV) and the anterior commissure (AC) were used as landmarks. MA, medial division of BST, anterior; LD, lateral division of BST, dorsal. Scale bar, 500 μm. **b**, Quantifications of Zif268-positive cells in the BST. 2MB-acid- and TMT-induced Zif268-positive cells in the BST-MA (MA) and BST-LD (LD) were counted for each brain section shown in **a**. Mean densities of activated cells (Zif268-positive cells per mm^2) ± s.e.m. were compared between the wild-type (white) and ΔD (grey) mice. Asterisk, $P < 0.05$. **c**, Measurements of the 2MB-acid- and TMT-induced rise in plasma ACTH. The plasma ACTH induced by 2MB acid, TMT or double-distilled water (DDW) was measured in the wild-type and ΔD mice. Average concentrations (pg ml^{-1}) ± s.e.m. of the plasma ACTH are shown. Asterisk, $P < 0.05$. **d**, A schematic diagram of the neural pathways in the mouse brain. A predator's odorant, TMT, activates two sets of glomeruli, one in the D domain and the other in the V domain of the olfactory bulb. We propose that TMT activates two different neuronal pathways: one for the innate fear response (blue) and the other for the odour–reward association learning (red). For TMT, the D-domain glomeruli activate the olfactory cortex (OC), and, subsequently, the BST-MA, which is thought to activate the HPA axis and increase the plasma ACTH concentration. The V-domain glomeruli are assumed to activate the BST-LD (LD) by means of the olfactory cortex responding to TMT. AG, adrenal gland; Hy., hypothalamus; LV, lateral ventricle; Pit., pituitary gland; OB, olfactory bulb; OE, olfactory epithelium.

the vacant areas in the olfactory bulb. These findings were unexpected, because in other sensory systems, such as retino-tectal projection[31] and barrel formation[32], competing axons eventually occupy vacant projection sites. In the olfactory system, the olfactory bulb may not simply be a projection screen to form a glomerular map, but may, instead, have area-specific functions that are predetermined genetically before the onset of OSN projection.

The present results indicate that D-domain glomeruli and V-domain glomeruli have separate roles in eliciting avoidance behaviours, by sending distinct signals to the brain (Fig. 5d). However, we must be careful in interpreting the data of behavioural tests. It is possible that ΔD mice require more time to recognize the qualities of odorants in the innate preference tests. It has been reported that there is a trade-off between speed and accuracy in rodent olfactory recognition[33–35]. We should consider the possibility that investigation times for aversive smells could be increased in the ΔD mice, if the V-domain glomeruli are slower to transmit odour information to the brain than the D-domain glomeruli. However, we believe that this is unlikely, because investigation times were decreased for the ΔD mice with attractive odorants (Fig. 3a). Even when the ΔD mice were exposed to TMT or 2MB acid for as long as 10–30 min, they did not demonstrate any increase in the levels of ACTH or Zif268 (Fig. 5a–c). Furthermore, ΔD mice found hidden odours more quickly than wild-type mice (Supplementary Fig. 11). From these results, it is difficult to explain the behavioural phenotypes of the ΔD mice in terms of the speed–accuracy trade-off. It is known that behavioural responses to odorants are affected by their concentrations. There is a possibility that, in the ΔD mice, detection thresholds for odorants are altered. For 2MB acid, the detection threshold was ten times higher for the ΔD mice than for the wild-type mice (Supplementary Figs 5b and 10). However, in the innate preference test using serially diluted 2MB acid, the ΔD mice were consistently on the attractive side whereas the wild-type mice were on the avoidance side (Fig. 3c). From these results, it is difficult to explain the behavioural abnormalities in ΔD mice only by detection thresholds.

In contrast to the ΔD mutant, ΔII mice showed aversive behaviour towards 2MB acid and iso-amyl amine. It seems that D-domain glomeruli are necessary and sufficient to induce aversive responses towards 2MB acid and iso-amyl amine. Because these odorants activate multiple sets of glomeruli in the D and V domains simultaneously, it was thought that these glomeruli would contribute equally to the processing of odour information in the glomerular map. However, the present study indicates that the mouse main olfactory system may be composed of at least two functional modules: one for innate odour responses and the other for discrimination and associative learning of complex odorous information. Innate aversive/fear responses probably involve genetically programmed neural circuits, like in the mammalian gustatory system[36,37], and in the chemosensory systems in *Drosophila melanogaster*[38,39] and *Caenorhabditis elegans*[40,41]. Like the immune system, the mouse olfactory system seems to have maintained innate odour responses with hard-wired neural circuits, in parallel with newly acquired discrimination/adaptive circuits.

METHODS SUMMARY

Mice. The ΔD and ΔII mice were generated by crossing the *Eno2-STOP-DTA* mouse with the *O-MACS→cre* mouse and *MOR23→cre* mouse, respectively. The class II-GFP mouse was generated by crossing the *MOR23→cre* mouse with the *ROSA-STOP-GFP* mouse.

Histology. *In situ* hybridization was performed as described[8,9]. For fluorescence immunohistochemistry, coronal sections of the brains, which were fixed with 4% paraformaldehyde in PBS for 5 min and rinsed in TBS-T (50 mM Tris, 150 mM NaCl and 0.2% Triton-X100), were then blocked with 10% normal goat

serum in TBS-T, and incubated with primary antibodies at 23 °C for 12–16 h. Sections were washed in TBS-T, and incubated with secondary antibodies.

Mapping odour-evoked activities. Adult male mice were habituated to the cage for 2 h, and then filter paper scented with test odorants was presented for 30 min. After 1 h, mice were killed and perfused with 4% paraformaldehyde in PBS. Zif268 mapping was performed as described with minor modifications[17].

Innate olfactory preference test. Adult ΔD and littermate mice ($n = 110$ for each genotype, and $n \geq 6$ for each test) were used in the test. To avoid confounding of data owing to learning, mice were used only once.

After habituating to the experimental environment, mice were transferred to the test cage, and a filter paper scented with a test odorant was introduced. Investigation times for the filter paper during the 3-min test period were measured.

Innate olfactory avoidance test. The ΔD, ΔII and wild-type littermates (adult male) ($n = 26$ for each genotype, and $n \geq 6$ for each test) were used in the test. The test cage was divided into two compartments (1:3) with a partition curtain. A filter paper scented with test odorant was introduced into the smaller compartment. Times (seconds) spent in the larger compartment were measured.

Full Methods and any associated references are available in the online version of the paper at www.nature.com/nature.

Received 3 August; accepted 14 September 2007.
Published online 7 November 2007.

1. Buck, L. & Axel, R. A novel multigene family may encode odorant receptors: a molecular basis for odor recognition. *Cell* **65,** 175–187 (1991).
2. Serizawa, S., Miyamichi, K. & Sakano, H. One neuron–one receptor rule in the mouse olfactory system. *Trends Genet.* **20,** 648–653 (2004).
3. Mombaerts, P. *et al.* Visualizing an olfactory sensory map. *Cell* **87,** 675–686 (1996).
4. Yoshihara, Y. *et al.* OCAM: a new member of the neural cell adhesion molecule family related to zone-to-zone projection of olfactory and vomeronasal axons. *J. Neurosci.* **17,** 5830–5842 (1997).
5. Oka, Y. *et al.* O-MACS, a novel member of the medium-chain acyl-CoA synthetase family, specifically expressed in the olfactory epithelium in a zone-specific manner. *Eur. J. Biochem.* **270,** 1995–2004 (2003).
6. Zhang, X. & Firestein, S. The olfactory receptor gene superfamily of the mouse. *Nature Neurosci.* **5,** 124–133 (2002).
7. Zhang, X. *et al.* High-throughput microarray detection of olfactory receptor gene expression in the mouse. *Proc. Natl Acad. Sci. USA* **101,** 14168–14173 (2004).
8. Tsuboi, A., Miyazaki, T., Imai, T. & Sakano, H. Olfactory sensory neurons expressing class I odorant receptors converge their axons on an antero-dorsal domain of the olfactory bulb in the mouse. *Eur. J. Neurosci.* **23,** 1436–1444 (2006).
9. Miyamichi, K., Serizawa, S., Kimura, H. M. & Sakano, H. Continuous and overlapping expression domains of odorant receptor genes in the olfactory epithelium determine the dorsal/ventral positioning of glomeruli in the olfactory bulb. *J. Neurosci.* **25,** 3586–3592 (2005).
10. Mori, K., Takahashi, Y. K., Igarashi, K. M. & Yamaguchi, M. Maps of odorant molecular features in the Mammalian olfactory bulb. *Physiol. Rev.* **86,** 409–433 (2006).
11. Malnic, B., Hirono, J., Sato, T. & Buck, L. B. Combinatorial receptor codes for odors. *Cell* **96,** 713–723 (1999).
12. Gogos, J. A., Osborne, J., Nemes, A., Mendelsohn, M. & Axel, R. Genetic ablation and restoration of the olfactory topographic map. *Cell* **103,** 609–620 (2000).
13. Imai, T., Suzuki, M. & Sakano, H. Odorant receptor-derived cAMP signals direct axonal targeting. *Science* **314,** 657–661 (2006).
14. Rubin, B. D. & Katz, L. C. Optical imaging of odorant representations in the mammalian olfactory bulb. *Neuron* **23,** 499–511 (1999).
15. Uchida, N., Takahashi, Y. K., Tanifuji, M. & Mori, K. Odor maps in the mammalian olfactory bulb: domain organization and odorant structural features. *Nature Neurosci.* **3,** 1035–1043 (2000).
16. Gurden, H., Uchida, N. & Mainen, Z. F. Sensory-evoked intrinsic optical signals in the olfactory bulb are coupled to glutamate release and uptake. *Neuron* **52,** 335–345 (2006).
17. Inaki, K., Takahashi, Y. K., Nagayama, S. & Mori, K. Molecular-feature domains with posterodorsal–anteroventral polarity in the symmetrical sensory maps of the mouse olfactory bulb: mapping of odourant-induced Zif268 expression. *Eur. J. Neurosci.* **15,** 1563–1574 (2002).
18. Vernet-Maury, E., Polak, E. H. & Demael, A. Structure–activity relationship of stress-inducing odorants in the rat. *J. Chem. Ecol.* **10,** 1007–1018 (1984).
19. Hebb, A. L. *et al.* Odor-induced variation in anxiety-like behavior in mice is associated with discrete and differential effects on mesocorticolimbic cholecystokinin mRNA expression. *Neuropsychopharmacology* **27,** 744–755 (2002).
20. Hebb, A. L. *et al.* Brief exposure to predator odor and resultant anxiety enhances mesocorticolimbic activity and enkephalin expression in CD-1 mice. *Eur. J. Neurosci.* **20,** 2415–2429 (2004).
21. Ferguson, J. N. *et al.* Social amnesia in mice lacking the oxytocin gene. *Nature Genet.* **25,** 284–288 (2000).
22. Johnson, B. A. & Leon, M. Modular glomerular representations of odorants in the rat olfactory bulb and the effects of stimulus concentration. *J. Comp. Neurol.* **422,** 496–509 (2000).
23. Wood, R. W. & Coleman, J. B. Behavioral evaluation of the irritant properties of formaldehyde. *Toxicol. Appl. Pharmacol.* **130,** 67–72 (1995).
24. Dielenberg, R. A. & McGregor, I. S. Defensive behavior in rats towards predatory odors: a review. *Neurosci. Behavi. Rev.* **25,** 597–609 (2001).
25. Nyby, J., Kay, E., Bean, N. J., Dahinden, Z. & Kerchner, M. Male mouse attraction to airborn urinary odors of conspecific and to food odors; effects of food deprivation. *J. Comp. Psychol.* **99,** 479–490 (1985).
26. Kay, E. & Nyby, J. LiCl aversive conditioning has transitory effects on pheromonal responsiveness in male house mice (*Mus domesticus*). *Physiol. Behav.* **52,** 105–113 (1992).
27. Schellinck, H. M., Forestell, C. A. & LoLordo, V. M. A simple and reliable test of olfactory learning and memory in mice. *Chem. Senses* **26,** 663–672 (2001).
28. Day, H. E., Masini, C. V. & Campeau, S. The pattern of brain *c-fos* mRNA induced by a component of fox odor; 2,5-dihydro-2,4,5-trimethylthiazoline (TMT), in rats, suggests both systemic and processive stress characteristics. *Brain Res.* **1025,** 139–151 (2004).
29. Wallece, K. J. & Rosen, J. B. Neurotoxic lesions of the lateral nucleus of the amygdala decrease conditioned fear but not unconditioned fear of a predator odor: comparison with electrolytic lesions. *J. Neurosci.* **21,** 3619–3627 (2001).
30. Fendt, M., Endres, T. & Apfelbach, R. Temporary inactivation of the bed nucleus of the stria terminalis but not the amygdale blocks freezing induced by trimethylthiazoline, a component of fox feces. *J. Neurosci.* **23,** 23–28 (2003).
31. Horder, T. J. Retention, by fish optic nerve fibres regenerating to new terminal sites in the tectum, of 'chemospecific' affinity for their original sites. *J. Physiol. (Lond.)* **6,** 53P–55P (1971).
32. Van der Loos, H. & Woolsey, T. A. Somatosensory cortex: structural alterations following early injury to sense organs. *Science* **179,** 395–398 (1973).
33. Uchida, N. & Mainen, Z. F. Speed and accuracy of olfactory discrimination in the rat. *Nature Neurosci.* **6,** 1224–1229 (2003).
34. Abraham, N. M. *et al.* Maintaining accuracy at the expense of speed: stimulus similarity defines odor discrimination time in mice. *Neuron* **44,** 865–876 (2004).
35. Rinberg, D., Koulakov, A. & Gelperin, A. Speed–accuracy tradeoff in olfaction. *Neuron* **51,** 351–358 (2006).
36. Zhao, G. Q. *et al.* The receptors for mammalian sweet and umami taste. *Cell* **115,** 255–266 (2003).
37. Huang, A. L. *et al.* The cells and logic for mammalian sour taste detection. *Nature* **442,** 934–938 (2006).
38. Suh, G. S. *et al.* A single population of olfactory sensory neurons mediates an innate avoidance behaviour in *Drosophila. Nature* **431,** 854–859 (2004).
39. Stockinger, P., Kvitsiani, D., Rotkopf, S., Tirian, L. & Dickson, B. J. Neural circuitry that governs *Drosophila* male courtship behavior. *Cell* **121,** 795–807 (2005).
40. Troemel, E. R., Kimmel, B. E. & Bargmann, C. I. Reprogramming chemotaxis responses: sensory neurons define olfactory preferences in *C. elegans. Cell* **91,** 161–169 (1997).
41. Tobin, D. *et al.* Combinatorial expression of TRPV channel proteins defines their sensory functions and subcellular localization in *C. elegans* neurons. *Neuron* **35,** 307–318 (2002).
42. Shimshek, D. R. *et al.* Codon-improved Cre recombinase (iCre) expression in the mouse. *Genesis* **32,** 19–26 (2002).
43. Feng, G. *et al.* Imaging neuronal subsets in transgenic mice expressing multiple spectral variants of GFP. *Neuron* **28,** 41–51 (2000).
44. Serizawa, S. *et al.* Mutually exclusive expression of odorant receptor transgenes. *Nature Neurosci.* **3,** 687–693 (2000).

Supplementary Information is linked to the online version of the paper at www.nature.com/nature.

Acknowledgements We thank R. Sprengel for the pBS-iCre vector, J. R. Sanes for the *Thy1-YFP*-G mouse and Tama Zoo for the snow leopard's urine. We also thank Y. Maruyama and A. Kawai for technical assistance. We are grateful to P. Mombaerts, J. Ngai, T. Yamamori and members of our laboratory for comments. This work was supported by the CREST program of the Japan Science and Technology Agency; the Mitsubishi Foundation; and the Special Promotion Research Grant from the Ministry of Education, Science and Culture of Japan. R.K. is supported by the PRESTO program of the Japan Science and Technology Agency.

Author Contributions K.K. and R.K. planned and performed most of the experiments. Optical imaging of intrinsic signals and mitral cell labelling were done by H.M. and K.M. Y.O. participated in the initial characterization of the *O-MACS→cre* knock-in mouse. T. Imai generated the *MOR23→cre* transgenic mouse. M.I. and M.O. helped generate the *O-MACS→cre* mouse. T. Ikeda and S.I. generated the *Eno2-STOP-DTA* mouse. T.K. advised on the behavioral analysis. H.S. supervised the project. The manuscript was written by K.K., R.K. and H.S.

Author Information Reprints and permissions information is available at www.nature.com/reprints. Correspondence and requests for materials should be addressed to H.S. (sakano@mail.ecc.u-tokyo.ac.jp).

METHODS

Mice. To generate the *O-MACS→cre* mice, a 1.3-kilobase (kb) fragment just upstream of the start codon of the *O-MACS* gene and a 6.9-kb fragment containing exon 2 and exon 3 of *O-MACS* were amplified by PCR from the mouse genome, and subcloned into pBluescript (Stratagene), containing the herpes simplex virus thymidine kinase (*hsv-tk*) gene. The SV40-polyA was amplified by PCR from pEGFP-N1 (Clontech), and integrated downstream of the codon-improved Cre recombinase (*iCre*) gene in pBlue.iCre[42]. The resulting iCre-SV40 polyA sequence was integrated in-frame into the ATG site of the *O-MACS* gene. The phosphoglycerate kinase 1 (pgk)-Neo-polyA sequence flanked by two FLP recognition targets (FRTs) derived from pPGK-neo-FRT (Gene Bridges), was inserted downstream of the iCre-polyA. The resulting targeting construct was transfected into embryonic stem cells, D3. Generation of the *MOR23→cre* transgenic mice has been described[13]. The *Eno2-STOP-DTA* mouse (T. Ikeda and S.I., unpublished observations) will be described elsewhere. The *ROSA-STOP-lacZ* (stock number 3309) and *ROSA-STOP-GFP* (stock number 4077) reporter mice were purchased from The Jackson Laboratory. The *Thy1-YFP-G*[43] mouse (Supplementary Fig. 8) was provided by J. R. Sanes. The *O-MACS→cre* knock-in mouse is in a mixed background of C57BL6 and 129Svj. Both *MOR23→cre* and *Eno2-STOP-DTA* mice are of the C57BL6 background. For behavioural analyses, the wild-type littermates were used as controls.

Histology. *In situ* hybridization was performed as described[8,9]. Antisense RNA probes for the odorant receptor genes[8,9] and *O-MACS*[5] were prepared as described. Other probes were prepared from the following open reading frame sequences by PCR: *V2r1b* (nucleotides 1,696–2,551), *V2r11* (also known as *Vmn2r89*, 1,599–2,941), *V2r15* (42–911), *V1re9* (710–1,396), *V1rj3* (279–821), *V1rg1* (100–732) and *Reln* (960–1,920). For fluorescence immunohistochemistry, coronal sections of the brains from animals, which were perfused with 4% paraformaldehyde, were fixed with 4% paraformaldehyde in PBS for 5 min and rinsed in TBS-T (50 mM Tris, 150 mM NaCl and 0.2% Triton-X100) three times. Samples were then blocked with 10% normal goat serum in TBS-T, and incubated with primary antibodies at room temperature (23 °C) overnight (12–16 h). Sections were washed in TBS-T three times, and incubated with secondary antibodies conjugated to Cy3 (1:200, Jackson ImmunoResearch), Alexa Fluor-488 (1:200, Molecular Probes) or Alexa Fluor-647 (1:200, Molecular Probes). The following primary antibodies were used: O-CAM (1:1,000)[4], GFP (1:100, Nacalai Tesque), synaptotagmin (1:500, Chemicon), Zif268 (1:500, Santa Cruz Biotechnology), GABA (1:2,000, Sigma) and tyrosine hydroxylase (1:200, Chemicon). For labelling of mitral cells, the dorsal surface of the olfactory bulb was surgically exposed, and a glass micropipette (filled with 2% neurobiotin in 1 M NaCl) was inserted vertically into the olfactory bulb. Positive current was applied for labelling the neuron (300–400 nA at 50% duty cycle of 7-s pulses for 30 min). The coronal olfactory bulb sections were dissected from the labelled animal and stained with the ABC kit (Vector Laboratories). Anatomical analyses of the olfactory epitheliums and olfactory bulbs of ΔD and ΔII mice will be described elsewhere (R.K. *et al.*, manuscript in preparation). X-gal (5-bromo-4-chloro-3-indolyl-β-D-galactoside) staining was performed as described[44].

Polymerase chain reaction with reverse transcription. DNase-treated total RNA extracted from the olfactory epithelium with the RNeasy kit (Qiagen) was used to prepare random-primed complementary DNA with Superscript III (Invitrogen). PCR primers have been described[8,9].

Mapping odour-evoked activities. Adult male mice were habituated to the cage for 2 h, and then filter paper scented with one of the following odorants was presented for 30 min: 2MB acid (870 μM), *n*-pentanal (370 μM) or TMT (1,200 μM). After 1 h, mice were killed and perfused with 4% paraformaldehyde in PBS. For Zif268 mapping, the published method[17] was modified. Consecutive coronal sections of the class II-GFP (wild-type) and ΔD mice ($n = 1$ for each condition) after the exposure to odorants, were immunostained with anti-Zif268 or anti-OCAM antibodies. The sections were also immunostained with anti-GFP and anti-synaptotagmin antibodies to identify the boundary of the D_I and D_{II} domains in the wild-type olfactory bulb. Zif268-positive and -negative glomeruli were mapped on the unrolled map. Boundaries between the D_{II} and V domains were identified by OCAM. For the Zif268 mapping in the BST, coronal sections were immunostained with anti-Zif268 antibodies. Zif268-positive cells were counted for both ΔD and wild-type mice ($n = 3$ for each genotype).

Unrolled maps of the olfactory bulb. Unrolled maps were constructed as described[15,17]. In brief, a smooth line was traced along the centre of the glomerular layer of immunostained coronal sections. The line was flattened by opening at the most ventro-lateral point. For glomerular arrangement (Fig. 2 and Supplementary Figs 4, 5a, 6 and 7), D_I-, D_{II}- and V-domain glomeruli were mapped on the flattened lines. For mapping the odour-evoked activities (Fig. 2), Zif268-positive and -negative glomeruli were mapped along the flattened lines. The unrolled map was generated by aligning the flattened traces of consecutive sections using the dorso-medial edge of the glomerular layer as a reference. For Supplementary Figs 6 and 7, the imaged region was determined with reference to the dye-injected points, and superimposed onto the map.

Optical imaging of intrinsic signals. Imaging and marker-dye injections were performed on adult, male, class II-GFP ($n = 2$) and ΔD ($n = 3$) mice as described[15]. Consecutive coronal sections of olfactory bulb from imaged animals were immunostained with anti-OCAM, anti-GFP and anti-synaptotagmin antibodies. Dorsal views of glomeruli in the D_I domain ($GFP^-/OCAM^-$), D_{II} domain ($GFP^+/OCAM^-$) and V domain ($OCAM^+$) were constructed and superimposed onto the optical imaging signals using dye-injected points as references.

Olfactory habituation–dishabituation test. The test was performed as described[21] with minor modifications using adult littermates ($n = 59$ for ΔD and $n = 61$ for wild type; $n \geq 6$ for each test). Mice were habituated to the cage (20 × 15 × 13 cm), and then a filter paper (2 × 2 cm) with 20 μl of distilled water was presented for 3 min. This was repeated three times with 1-min intervals. On the fourth trial, a filter paper with the indicated amount of the test odorant was presented for 3 min. Investigation times during the 3-min test period were measured on the third and fourth trials. The mouse behaviour was recorded with a digital video camera (30 frames per second, 640 × 480 pixels) for the analysis. We defined 'an investigation' as a nasal contact with the filter paper within a 1 mm distance.

Innate olfactory preference test. Adult ΔD and littermate mice ($n = 110$ for each genotype, and $n \geq 6$ for each test) were used in the test. To avoid confounding of data owing to learning, mice were used only once. To habituate to the experimental environment, mice were placed individually in a cage that was identical to the test cage (20 × 15 × 13 cm). After 30 min of habituation, mice were transferred to a new cage. This habituation was repeated four times for each animal. Soon after the habituation, mice were transferred to the test cage, and a filter paper (2 × 2 cm) scented with a test odorant was introduced. Investigation times for the filter paper during the 3-min test period were measured. The mouse behaviour was recorded with a digital video camera for the analysis. Odorants used were: guaiacol (158 μM), eugenol (128 μM), vanillin (64 μM), 2MB acid (174 μM), cyclobutanecarboxylic acid (206 μM), iso-amyl amine (16.8 μM), *n*-pentanal (74 μM), hexanal (156 μM), 2-hexanone (158 μM, Tokyo chemical industry), TMT (314 μM, Pherotech), peanut butter (10% w/v, 40 μl), urine of female mice (20 μl) and snow leopard urine (20 μl). Aversion conditioning with LiCl was adapted from the published procedure[42] as follows. The ΔD mouse ($n = 36$, and $n = 6$ for each test) was first exposed to test odorants for 3 min as described for the innate olfactory preference test. For aversive conditioning, 0.5 M LiCl solution was immediately injected (20 ml kg^{-1}) into the peritoneal cavity. After 2 days, the mice were subjected to the olfactory preference test with the same odorants, and investigation times (seconds) were measured.

Innate olfactory avoidance test. The ΔD, ΔII and wild-type littermates (adult male) ($n = 26$ for each genotype, and $n \geq 6$ for each test) were used in the test. To avoid confounding owing to learning, each mouse was used only once in the test. The test cage (20 × 15 × 13 cm) was divided into two compartments (1:3) with a partition curtain. Mice could move freely between the two compartments. The mice were habituated to the cage for ~10 min, and then a filter paper scented with 20 μl test odorant was introduced into the smaller compartment. Times (seconds) spent in the larger compartment were measured during the 3-min test period. Avoidance times were recorded as the time spent in the larger compartment for each odorant subtracted by the time spent for distilled water. The mouse behaviour was recorded with a digital video camera for the analysis. Odorants used were 2MB acid (8.7 M), iso-amyl amine (8.4 M) and TMT (15.7 M).

Olfactory discrimination test. The test was performed as described[27] with minor modifications. The ΔD and wild-type littermates (adult male) ($n = 24$ for each genotype, $n = 6$ for each test) were tested. The mice were food-restricted to maintain 80–85% of their free feeding weights and trained to associate one of the two related odorants with the sugar reward for 4 days. During the training, the mice received four 10-min trials a day: two trials for an odour paired with sugar reward and two for the unpaired odour. On day five, each test odorant was placed independently, without sugar, in the cage (26 × 40 × 18 cm) with bedding (~4,000 cm^3). The mouse behaviour was recorded with a digital video camera for the analysis. The time (seconds) spent digging for each odorant was measured during the 2-min test period. Odorant concentrations were: 2MB acid (8.7 M), cyclobutanecarboxylic acid (10.3 M), *n*-pentanal (3.7 M), hexanal (7.8 M), eugenol (6.4 M), (−)carvone (6.3 M, Tokyo chemical industry), (+)carvone (6.2 M, Tokyo chemical industry) and TMT (15.7 M). For each odorant, 20 μl was used.

ACTH assay. The ACTH assay was adapted from the published procedure[28]. The ΔD and wild-type littermates (10–12-week-old male) were used ($n = 24$ for each genotype, $n = 8$ for each analysis). The mice were housed individually to avoid

the elevation of plasma ACTH owing to fighting. Mice were maintained with 12:12 h light:dark schedule (lights turned on at 9:00). Odour presentation and blood sampling were performed between 10:00 and 11:00. Filter paper, scented with either double-distilled water or TMT (77.6 μl each), was quietly dropped into the cage with great care not to excite the animal. After exposure to the odorant for 10 min, the mice were decapitated quickly (within 15 s of removing them from their cages), and blood samples were collected. Plasma ACTH concentrations were measured using the ACTH ELISA kit (MD Biosciences).

Statistics. Data are presented as mean ± s.e.m. Statistical analysis was performed using a Student's *t*-test. The criterion for statistical significance is $P < 0.05$ in all cases.